DOI: 10.1002/ejic.200901188

[60]Fullerene–Metal Cluster Complexes: Understanding Novel η^1 and $\eta^{2[6:5]}$ Bonding Modes of Metallofullerenes

Young-Kyu Han,*[a] Kyoung Hoon Kim,[a] Jong Chan Kim,[a] Bo Keun Park,[b] and Joon T. Park*[b]

Keywords: Fullerenes / Transition metals / Bonding modes / Cluster compounds / Density functional calculations

We performed extensive density functional calculations on various metallofullerene complexes and their polyanions to gain insight into novel η^1 and $\eta^{2[6:5]}$ metal (M)–C_{60} bonding modes. For L_nMC_{60} (L = ligand), the η^1 mode is calculated to be the most stable, followed by $\eta^{2[6:5]}$ and $\eta^{2[6:6]}$ for –3 anions, in contrast to $\eta^{2[6:6]} >> \eta^{2[6:5]} \approx \eta^1$ for neutral cases. This observation is responsible for the transformation from $\eta^{2[6:6]}$ to η^1 for $L_nM_3C_{60}$, such as $[Os_3(CO)_9C_{60}]$, upon successive electron reductions. Our energy partitioning analysis (EPA) indicates that the π-type character of $\eta^{2[6:6]}$ is much larger than that of $\eta^{2[6:5]}$. An electron addition decreases the π-type interaction of both the $\eta^{2[6:6]}$ and $\eta^{2[6:5]}$ modes by about 35 %, whereas it has little effect on σ-type interactions. Because of the large proportion of π-character in $\eta^{2[6:6]}$ coordination, the stability of $\eta^{2[6:6]}$ coordination decreases steeply as electron reductions continue. On the basis of the EPA results, we could explain why the reaction of $[Os_3(CO)_8(CNR)(\mu_3\text{-}\eta^{2[6:6]},\eta^{2[6:6]},\eta^{2[6:6]}\text{-}C_{60})]$ (R = CH_2Ph) with CNR (4e donor) produces $[Os_3(CO)_8(CNR)(\mu_3\text{-}CNR)(\mu_3\text{-}\eta^1,\eta^{2[6:5]},\eta^1\text{-}C_{60})]$. The η^1 and $\eta^{2[6:5]}$ bonding modes of M–C_{60} are crucial to fully understand the bonding nature of M–C_{60} bonds in exohedral metallofullerene complexes.

Introduction

Considerable research effort has been devoted to creating a variety of [60]fullerene-based (C_{60}) derivatives. Their numerous applications in materials science include optical, magnetic, electronic, catalytic, and biological applications.[1–8] In particular, many researchers have examined exohedral metallofullerene complexes to investigate and understand the effects of metal (M) coordination on the chemical and physical properties of C_{60}, as well as the reactivities and electrochemical properties of these complexes, ultimately to develop new electronic nanomaterials and nanodevices.[9–14] Although every carbon atom in C_{60} is chemically equivalent, the structure of C_{60} offers many different possible bonding sites and modes of interaction with metals. These sites are (1) directly over a single carbon atom (representing η^1-coordination), (2) above the midpoint of a 6:6 ring junction (η^2-coordination, $\eta^{2[6:6]}$), (3) above the midpoint of a 6:5 ring junction ($\eta^{2[6:5]}$), (4) above the center of a pentagonal face (η^5-coordination), and (5) above the center of a hexagonal face (η^6-coordination) (see Figure 1). Continuous development in metal–C_{60} chemistry led to the synthesis of various metallofullerene complexes with η^1-,[15] η^2-,[10,16–22] η^5-,[23–25] and η^6-bonding modes[26], but peculiar chemistry is dominated by π-type M–C_{60} interactions, as a metal atom is attached in an η^2 fashion to a [6:6] bond in C_{60}. There have been various metallofullerene complexes

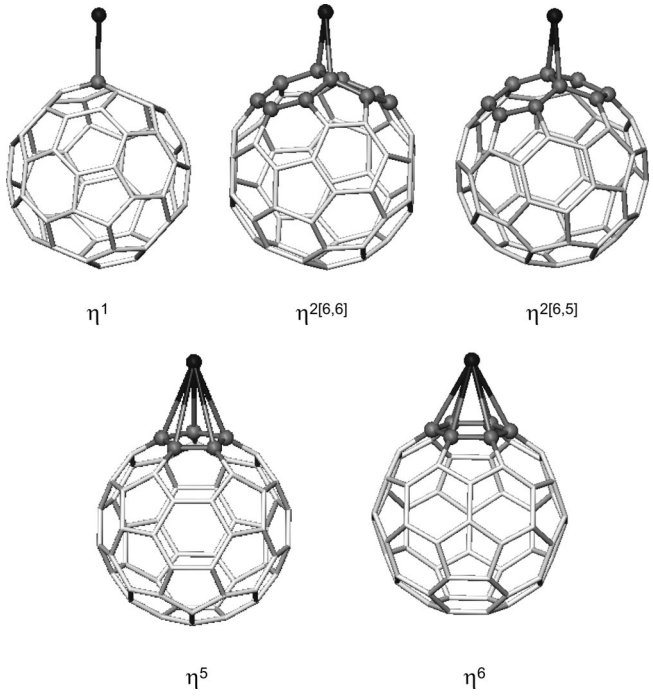

Figure 1. Five possible metal–C_{60} bonding modes.

[a] Corporate R&D, LG Chem. Ltd. Research Park, Daejeon 305-380, South Korea
[b] Department of Chemistry and School of Molecular Science (BK 21), Korea Advanced Institute of Science and Technology (KAIST), Daejeon 305-701, South Korea
E-mail: ykhan@lgchem.com
joontpark@kaist.ac.kr

Supporting information for this article is available on the WWW under http://dx.doi.org/10.1002/ejic.200901188.

with an $\eta^{2[6:6]}$ M–C_{60} bond across the periodic table.[10,16–22] The chemistry of metal–C_{60} cluster σ complexes has remained relatively unexplored, although such complexes are very important in the selective functionalization of C_{60}.[22,27–31] Herein, we show that the η^1 and $\eta^{2[6:5]}$ bonding modes of M–C_{60} are crucial to fully understanding the bonding nature of M–C_{60} bonds in exohedral metallofullerene complexes.

Shapley et al.[32–34] and Park et al.[35–39] independently prepared various $L_nM_x(C_{60})_y$ complexes and demonstrated that a variety of cluster frameworks [$Re_3(\mu\text{-}H)_3$, Ru_3, Os_3, Ru_5C, Os_5C, $PtRu_5C$, Ru_6C, and Ru_6] can bind to C_{60} through a face-capping cyclohexatriene-like bonding mode: μ_3-η^2,η^2,η^2-C_{60}. The metallofullerene complexes with this relatively strong bonding mode exhibited remarkable thermal and electrochemical stabilities, uniquely suitable for various device applications, which is in contrast to other previously known η^2-C_{60} metal cluster complexes.[11] Park et al.[35,38] demonstrated an interesting strong electronic communication between C_{60} and metal cluster centers that can be readily fine-tuned by controlling the electronic properties of the attached ligands on the metal cluster center. Electrochemical studies of C_{60} derivatives of Ir_4 and Rh_6 clusters have also revealed strong electronic interactions between C_{60} cages, through the metal cluster spacers.[13] Park et al.[12] reported a highly ordered [60]fullerene triosmium cluster–zinc porphyrin dyad self-assembled monolayer (SAM) on an indium–tin oxide surface. These exhibited the highest photocurrent generation efficiency (19.5%) reported for dyad photovoltaic cells based on SAMs.

Park et al.[40] reported the first example of an η^2 (π-type) to η^1 (σ-type) conversion in a neutral [$L_nOs_3C_{60}$] complex; the authors demonstrated the transformation of the bonding mode of C_{60} on an Os_3 framework by using X-ray crystallography, from the μ_3-η^2,η^2,η^2 bonding mode to the μ_3-η^1,η^2,η^1 bonding mode, which was induced by an external ligand. It is very interesting that the μ_3-$\eta^{2[6:6]}$,$\eta^{2[6:6]}$,$\eta^{2[6:6]}$ bonding mode was transformed into the μ_3-η^1,$\eta^{2[6:5]}$,η^1 mode, but the origin is unknown. Kim et al.[41] predicted from their density functional calculations for μ_3-η^2,η^2,η^2 [$Os_3(CO)_9C_{60}$] that the transformation of the μ_3-η^2,η^2,η^2 mode (neutral) into the μ_3-η^2,η^1,η^1 (–4 anion) bonding mode of C_{60} can occur only by electron reductions. In this study, we performed extensive density functional calculations on various L_nMC_{60} and $L_nM_3C_{60}$ complexes and their polyanions to gain insight into novel η^1 and $\eta^{2[6:5]}$ M–C_{60} bonding modes.

Computational Details

Our calculations were based on density functional theory (DFT) at the generalized gradient approximation (GGA) level (employing Becke's 1988 functional for exchange and Perdew–Wang's 1991 functional for correlation: BPW91[42,43]). The energy-consistent relativistic effective core potential (RECP)[44] was used for the metal atoms. Double numerical plus polarization (DNP) basis sets were also used for C, N, O, and H atoms. All metal–C_{60} complexes were optimized for the neutral and anionic states. Various multiplicities were considered: the closed-shell and open-shell species are singlet and doublet, respectively. The vibrational frequencies were calculated at the optimized geometries for $L_nM_3C_{60}$ to confirm that the structures are true local minima. The following convergence criteria (all given in atomic units) were imposed: energy, 2×10^{-5}; maximum gradient, 4×10^{-3}; and maximum displacement, 5×10^{-3}. All calculations were performed by using Accelrys' DFT program DMol3.[45,46]

The nature of the metal–C_{60} bonding was investigated at the optimized geometries by DMol3 through the energy partitioning analysis (EPA) of the program package ADF, based on the EPA method of Morokuma and Ziegler.[47–49] The bond energy can be decomposed into contributions from three terms: $\Delta E = \Delta E_{prep} + \Delta E_{ster} + \Delta E_{orb}$

The preparation energy (ΔE_{prep}) is the energy necessary to deform the bonding moieties from their respective isolated equilibrium geometries into the geometries they assume in the bound complex. The steric energy (ΔE_{ster}) is the sum of two terms, one corresponding to the electrostatic interaction (ΔE_{elst}) between the fragments and the other to the Pauli repulsion energy (ΔE_{pauli}). ΔE_{ster} should not be confused with the loosely defined steric interaction between substituents in a molecule. The orbital interaction energy (ΔE_{orb}) is the energy due to the attractive interactions between occupied orbitals of one fragment and empty orbitals of the other fragment, as well as between the occupied and empty orbitals within a given fragment (polarization). The bonding analysis was carried out at the BPW91/TZP level of theory. The a′ orbital interactions of the complexes with C_s symmetry correspond to σ and $\pi_\perp$, and the a′′ interactions correspond to $\pi_\parallel$ and δ. The a′ and a′′ contributions can be regarded as σ and π interactions, because the contribution of $\pi_\perp$ and δ orbital interactions can safely be assumed to be small.[50]

Results and Discussion

We evaluated the relative energies for the $\eta^{2[6:6]}$, $\eta^{2[6:5]}$, η^1, η^5, and η^6 bonding modes of twelve L_nMC_{60} (M = Cr, Mo, W, Mn, Tc, Re, Fe, Ru, Os, Co, Rh, Ir; L = H, CO) complexes and their anions, where the neutral complexes comply with the 18-electron rule (see Table 1). The optimized structures of L_nMC_{60} are presented in the Supporting Information. The geometries were constrained to maintain the bonding modes. The geometries of the $\eta^{2[6,5]}$ and $\eta^{2[6,6]}$ complexes were optimized under C_s symmetry constraints. The geometries of the η^1, η^5, and η^6 complexes were optimized by constraining several dihedral angles. For instance, six dihedral angles were constrained to maintain the η^6 bonding mode. One of the dihedral angles was constituted by the metal atom, one C atom in the six-membered ring connected to the metal atom, and two C atoms in the opposite six-membered ring (see the Supporting Information). Because the η^5 and η^6 coordinations are very un-

Table 1. Relative energies (in kcal/mol) for the five bonding modes of L_nMC_{60} (M = Cr, Mo, W, Mn, Tc, Re, Fe, Ru, Os, Co, Rh, Ir; L = H, CO). The structures were optimized with geometry constraints (see the Supporting Information).

	neutral	–1	–2	–3	neutral	–1	–2	–3	neutral	–1	–2	–3
	$[Cr(CO)_5C_{60}]$				$[Mo(CO)_5C_{60}]$				$[W(CO)_5C_{60}]$			
$\eta^{2[6:5]}$	–1.1	–0.5	0.5	0.7	–2.0	–1.2	0.6	0.4	–2.4	–1.2	1.0	1.2
$\eta^{2[6:6]}$	–7.8	–1.9	4.8	[a]	–8.7	–2.9	3.6	5.7	–9.7	–2.9	4.7	6.1
η^1	0.0	0.0	0.0	0.0	0.0	0.0	0.0	0.0	0.0	0.0	0.0	0.0
η^5	8.6	10.5	10.9	7.6	9.2	11.4	12.8	9.3	10.4	12.8	14.1	11.0
η^6	3.3	[a]	[a]	[a]	5.3	[a]	[a]	[a]	7.0	11.1	[a]	[a]
	$[MnH(CO)_4C_{60}]$				$[TcH(CO)_4C_{60}]$				$[ReH(CO)_4C_{60}]$			
$\eta^{2[6:5]}$	–2.1	–0.7	1.0	0.9	–2.3	–1.5	0.6	1.1	–2.6	–1.3	1.4	2.6
$\eta^{2[6:6]}$	–11.0	–4.4	2.9	6.7	–10.8	–5.0	2.3	5.6	–12.1	–5.5	3.0	6.8
η^1	0.0	0.0	0.0	0.0	0.0	0.0	0.0	0.0	0.0	0.0	0.0	0.0
η^5	10.0	12.3	13.6	10.0	9.8	11.8	13.5	10.6	11.7	13.9	16.2	[a]
η^6	5.5	[a]	[a]	[a]	5.4	[a]	[a]	[a]	7.9	11.7	11.7	[a]
	$[Fe(CO)_4C_{60}]$				$[Ru(CO)_4C_{60}]$				$[Os(CO)_4C_{60}]$			
$\eta^{2[6:5]}$	–2.8	–0.3	2.3	0.3	0.8	0.6	2.6	0.3	0.4	0.5	2.8	3.0
$\eta^{2[6:6]}$	–15.2	–7.2	1.6	6.6	–11.2	–5.6	2.2	6.3	–12.4	–6.4	2.3	7.3
η^1	0.0	0.0	0.0	0.0	0.0	0.0	0.0	0.0	0.0	0.0	0.0	0.0
η^5	10.5	10.3	8.0	[a]	9.6	8.6	7.7	[a]	11.1	9.8	8.5	[a]
η^6	10.4	11.3	[a]	[a]	9.1	9.6	5.4	[a]	10.1	10.5	9.0	[a]
	$[CoH(CO)_3C_{60}]$				$[RhH(CO)_3C_{60}]$				$[IrH(CO)_3C_{60}]$			
$\eta^{2[6:5]}$	–1.3	–0.4	1.4	3.0	1.0	0.8	2.2	2.1	1.8	1.4	3.2	4.1
$\eta^{2[6:6]}$	–11.9	–6.1	0.7	4.5	–7.8	–3.2	3.0	5.4	–10.2	–4.2	3.7	7.8
η^1	0.0	0.0	0.0	0.0	0.0	0.0	0.0	0.0	0.0	0.0	0.0	0.0
η^5	12.0	13.5	14.7	12.0	9.1	10.3	12.4	9.9	10.1	11.8	[a]	[a]
η^6	[a]	[a]	[a]	[a]	[a]	[a]	[a]	[a]	[a]	[a]	[a]	[a]

[a] Dissociated.

stable for all neutral and anion structures, we depicted the results only for the $\eta^{2[6:6]}$, $\eta^{2[6:5]}$, and η^1 bonding modes in Figure 2. For all neutral metallofullerene complexes, $\eta^{2[6:6]}$ coordination of C_{60} is the most stable, which is in harmony with the fact that the metallofullerene chemistry is dominated by $\eta^{2[6:6]}$ coordination of C_{60} to the metal center. It is worth noting that the successive addition of electrons to metallofullerene complexes significantly changes the relative energies of the three isomers. The stability of $\eta^{2[6:6]}$ coordination decreases steeply as electron reductions continue. Even for $Cr(CO)_5C_{60}$, complexes with $\eta^{2[6:6]}$ coordination are dissociated after the third electron reductions, whereas the $\eta^{2[6:5]}$ and η^1 structures exist as local minima. The η^1 mode is calculated to be the most stable, followed by $\eta^{2[6:5]}$ and $\eta^{2[6:6]}$ for –3 anions, in contrast to $\eta^{2[6:6]} >> \eta^{2[6:5]} \approx \eta^1$ for neutral cases. This observation seems to be responsible for the transformation from $\eta^{2[6:6]}$ to η^1 for $L_nM_3C_{60}$, such as $[Os_3(CO)_9C_{60}]$, upon successive electron reductions.[41] Although no X-ray structures for anionic $[L_nM_3C_{60}]$ (or $[L_nMC_{60}]$) complexes have been reported, cyclic voltammetry (CV) measurements have provided their reduction potentials for various $L_nM_3C_{60}$ complexes. We were able to reproduce the experimental CV data, with a small mean deviation of 0.02 V, for $[Os_3(CO)_9C_{60}]$ and $[Re_3H_3(CO)_9C_{60}]$, by using the density functional calculations of reduction potentials (see Table 2). CV modeling[51] for metallofullerene complexes is described in the Supporting Information. Our results for $[L_nM_3C_{60}]$ and $[L_nMC_{60}]$ complexes strongly imply that such $\eta^{2[6:6]}$ to η^1 conversions can occur in general $L_nM_x(C_{60})_y$-type metallofullerenes.

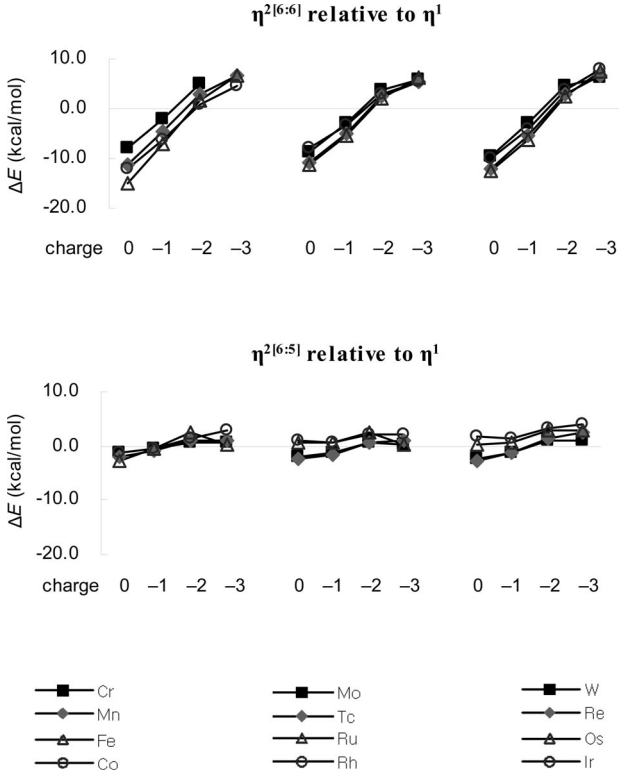

Figure 2. Relative energies (in kcal/mol) of $\eta^{2[6:6]}$ and $\eta^{2[6:5]}$ with respect to η^1. Optimized structures are given in the Supporting Information.

Table 2. Calculated reduction potentials (to the standard Fc/Fc^+ scale) for $[Os_3(CO)_9C_{60}]$ and $[Re_3H_3(CO)_9C_{60}]$.

	Bonding mode[a]	Charge	Calcd.[b]	Exp.[c]
$[Os_3(CO)_9C_{60}]$	(2,2,2)	0		
	(2,2,2)	–1	–0.97	–0.98
	(2,2,2)	–2	–1.29	–1.33
	(2,2,1)	–3	–1.65	–1.61
	(2,1,1)	–4	–1.73	–1.74
$[Re_3H_3(CO)_9C_{60}]$	(2,2,2)	0		
	(2,2,2)	–1	–0.91	–0.95
	(2,2,2)	–2	–1.21	–1.24
	(2,2,1)	–3	–1.36	–1.34
	(2,1,1)	–4	–1.73	–1.73

[a] (2,2,2) denotes the μ_3-η^2,η^2,η^2 bonding mode. [b] The calculated reduction potentials were improved relative to those in ref.[51] by searching for more stable structures of $[Os_3(CO)_9C_{60}]$, $[Re_3H_3(CO)_9C_{60}]$, and their anions. [c] Ref.[35,38]

Table 3. Energy partitioning analysis (in kcal/mol) of $[Os(CO)_4C_{60}]$ and $[Os(CO)_4C_{60}]^{-1}$.

	η^1	$\eta^{2[6:6]}$	$\eta^{2[6:5]}$	η^1	$\eta^{2[6:6]}$	$\eta^{2[6:5]}$
	$[Os(CO)_4C_{60}]$[a]			$[Os(CO)_4C_{60}]^{-1}$[b]		
D_e	–15.0	–30.1	–16.2	–20.0	–28.9	–20.6
ΔE_{prep}	10.8	28.1	21.2	10.8	20.5	13.7
ΔE_{ster}	40.6	59.2	48.6	32.5	46.2	32.6
ΔE_{pauli}	128.5	186.8	141.4	127.7	166.9	120.7
ΔE_{elst}	–88.0	–127.7	–92.8	–95.1	–120.8	–88.1
ΔE_{orb}	–66.3	–117.4	–86.0	–63.3	–95.5	–66.9
$\Delta E_{a'}(\sigma)$	*–60.6*	–45.9	–39.1	*–58.6*	–45.6	*–38.5*
$\Delta E_{a''}(\pi)$	–5.7	*–71.5*	*–46.9*	–4.7	*–49.9*	–28.4

[a] Main orbital interactions between the HOMOs of $Os(CO)_4$ and the LUMOs of C_{60} are presented in the Supporting Information. [b] The singly occupied molecular orbitals (SOMO) for the $\eta^{2[6:6]}$,$\eta^{2[6:5]}$ and $[\eta^1\text{-}Os(CO)_4C_{60}]^{-1}$ complexes are shown in the Supporting Information.

One can easily assume that the bonding nature of η^1 and η^2 modes is quite different. It is worth noting that the η^1 and $\eta^{2[6:5]}$ bond strengths become high, as electron reductions proceed, with respect to the corresponding $\eta^{2[6:6]}$ bond strength. To get a detailed insight into the nature of the M–C_{60} bond in the $[L_nMC_{60}]$ complexes, Os–C_{60} bonding analysis was performed for neutral and –1 anion $[Os(CO)_4C_{60}]$ complexes. It should be mentioned that the metallofullerene complexes containing Os metal atoms have been the most widely investigated in experiments.[11,14,32,33,35,37,52–55] The nature of M–C_{60} bonding has been investigated through energy partitioning analysis (EPA); the results are given in Table 3. The three top entries in Table 3 give the values of the dissociation energy D_e, ΔE_{prep}, ΔE_{ster}, and ΔE_{orb}. The attractive Os–C_{60} bonding comes mainly from ΔE_{orb}, rather than ΔE_{ster}. The orbital interactions having a′(σ) and a′′(π) symmetry can be distinguished by EPA calculations.[50] Table 3 clearly shows that the η^1 and η^2 modes are σ- and π-type, respectively, as expected. However, we stress that the π-type character of $\eta^{2[6:6]}$ (σ/π = 1:1.6) is much larger than that of $\eta^{2[6:5]}$ (σ/π = 1:1.2). An electron addition decreases the π-type interaction of both the $\eta^{2[6:6]}$ and $\eta^{2[6:5]}$ modes by about 35%, whereas it has little effect on σ-type interactions. Because of the large proportion of π-character in $\eta^{2[6:6]}$ coordination, the stabilities of $\eta^{2[6:6]}$ coordination decrease steeply as electron reductions continue. Even in the –1 anion state, the $\eta^{2[6:6]}$ and $\eta^{2[6:5]}$ bonding modes are π- and σ-dominant, respectively. As a result, the η^1 mode is the most stable, followed by $\eta^{2[6:5]}$ and $\eta^{2[6:6]}$ for the higher –3 anion complex. The EPA results reveal that the reason that the $\eta^{2[6:5]}$ mode is more stable than the $\eta^{2[6:6]}$ mode is the relatively large σ-character of the $\eta^{2[6:5]}$ mode, that is, the $\eta^{2[6:5]}$ mode is preferable to the $\eta^{2[6:6]}$ mode for electron-rich environments.

On the basis of the EPA results, we can expect that introduction of an electron-donating ligand to a metal cluster framework would cause the complexes to have η^1 or $\eta^{2[6:5]}$ M–C_{60} bonding modes, even in a neutral state. Actually, the reaction of $[Os_3(CO)_8(CNR)(\mu_3\text{-}\eta^{2[6:6]},\eta^{2[6:6]},\eta^{2[6:6]}\text{-}C_{60})]$ (R = CH_2Ph) (**1**) and CNR (4e donor) at 80 °C in chlorobenzene forms $[Os_3(CO)_8(CNR)(\mu_3\text{-}CNR)(\mu_3\text{-}\eta^1,\eta^{2[6:5]},\eta^1\text{-}C_{60})]$ (see Scheme 1).[40]

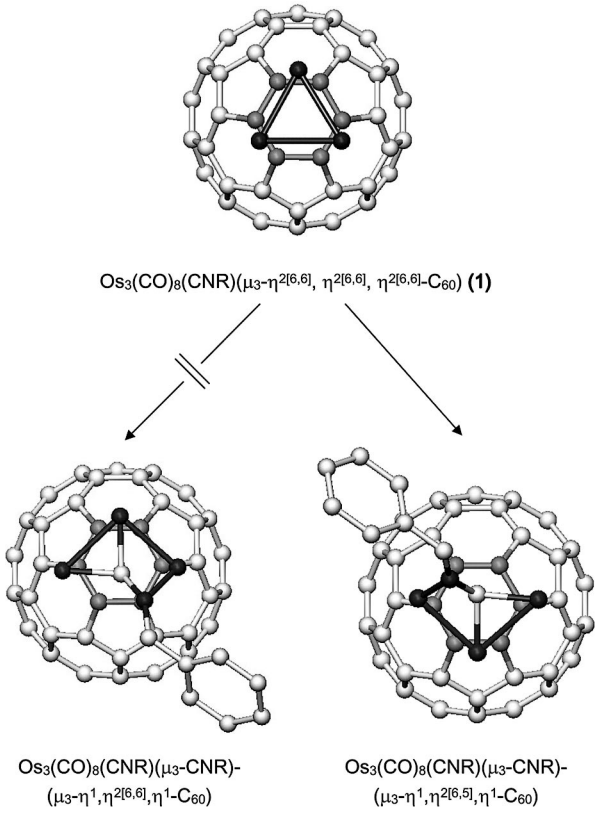

Scheme 1. Reaction of $[Os_3(CO)_8(CNR)(\mu_3\text{-}\eta^{2[6:6]},\eta^{2[6:6]},\eta^{2[6:6]}\text{-}C_{60})]$ (R = CH_2Ph) (**1**) with CNR.

We note that the transformation to the μ_3-η^1,$\eta^{2[6:5]}$,η^1 mode is very interesting because the transformation from μ_3-$\eta^{2[6:6]}$,$\eta^{2[6:6]}$,$\eta^{2[6:6]}$ to μ_3-η^1,$\eta^{2[6:6]}$,η^1 is more plausible than to μ_3-η^1,$\eta^{2[6:5]}$,η^1, as shown in Scheme 1. When the μ_3-CNR ligand is introduced, the Os_3 framework seems to be mobile on the C_{60} surface, and ultimately binds to C_{60} as the most stable form. We optimized the various low-lying

structures of the $[Os_3(CO)_8(CNR)(\mu_3\text{-}CNR)C_{60}]$ isomers. The results, along with the relative energies, are presented in Figure 3. More information on the optimized structures is presented in the Supporting Information. The experimentally observed $\mu_3\text{-}\eta^1,\eta^{2[6:5]},\eta^1$ isomer is calculated to be the most stable and is 4.9 kcal/mol more stable than the $\mu_3\text{-}\eta^1,\eta^{2[6:6]},\eta^1$ isomer. We could not obtain a stable $\mu_3\text{-}\eta^1,\eta^1,\eta^1$ isomer that was 29.7 kcal/mol higher than the $\mu_3\text{-}\eta^1,\eta^{2[6:5]},\eta^1$ isomer, which is ascribable to the distorted Os_3 framework resulting from the introduced μ_3-CNR ligand.

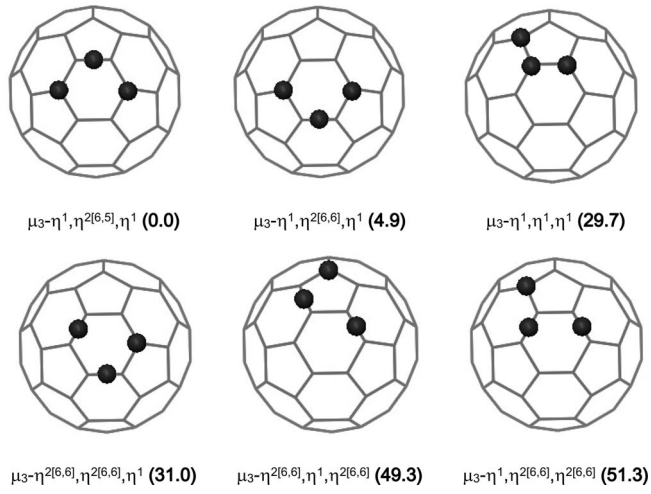

Figure 3. Relative energies (in kcal/mol) for $[Os_3(CO)_8(CNR)(\mu_3\text{-}CNR)C_{60}]$. ●: Osmium; CO and CNR ligands are omitted for clarity.

Conclusions

We have performed extensive density functional calculations on various $[L_nMC_{60}]$ and $[L_nM_3C_{60}]$ complexes and their polyanions to gain insight into novel η^1 and $\eta^{2[6:5]}$ M–C_{60} bonding modes. For $[L_nMC_{60}]$, the η^1 mode is calculated to be the most stable, followed by $\eta^{2[6:5]}$ and $\eta^{2[6:6]}$ for –3 anions, in contrast to $\eta^{2[6:6]} >> \eta^{2[6:5]} \approx \eta^1$ for neutral cases. This observation seems to be responsible for the transformation from $\eta^{2[6:6]}$ to η^1 for $[L_nM_3C_{60}]$, such as $[Os_3(CO)_9C_{60}]$, upon successive electron reductions. Our EPA calculations indicate that the π-type character of $\eta^{2[6:6]}$ is much larger than that of $\eta^{2[6:5]}$. The addition of an electron significantly decreases the π-type interaction of both the $\eta^{2[6:6]}$ and $\eta^{2[6:5]}$ modes, whereas it has little effect on σ-type interactions. Because of the large proportion of π-character of $\eta^{2[6:6]}$ coordination, the stability of $\eta^{2[6:6]}$ coordination decreases steeply as electron reductions continue. On the basis of the EPA results, we could explain why the reaction of $[Os_3(CO)_8(CNR)(\mu_3\text{-}\eta^{2[6:6]},\eta^{2[6:6]},\eta^{2[6:6]}\text{-}C_{60})]$ (R = CH_2Ph) with CNR (4e donor) produces $[Os_3(CO)_8(CNR)(\mu_3\text{-}CNR)(\mu_3\text{-}\eta^1,\eta^{2[6:5]},\eta^1\text{-}C_{60})]$.

In exohedral metallofullerene chemistry, understanding the η^1 and $\eta^{2[6:5]}$ bonding modes is as important as understanding the $\eta^{2[6:6]}$ mode. We have unraveled an aspect of C_{60}: its behavior as a versatile multifunctional ligand exhibits various σ- and π-bonding modes. Our finding could be helpful for the interpretation and understanding of the peculiar chemistry of transition-metal complexes with fullerenes.

Supporting Information (see footnote on the first page of this article): Optimized structures of L_nMC_{60}; SOMOs of the $Os(CO)_4\text{-}C_{60}^{-1}$ complexes; main occupied–unoccupied orbital interactions for the $Os(CO)_4C_{60}$ complexes; CV modeling for metallofullerene complexes.

Acknowledgments

This work was supported by the Korea Research Foundation, Korean Government (MOEHRD; KRF-2005-201-C00021) and by the Nano R&D Program of the Korea Science and Engineering Foundation (KOSEF) (grant 2005-02618) funded by MEST. This work was also supported in part by the SRC program (grant R11-2005-008-00000-0) of KOSEF through the Center for Intelligent Nano-Bio Materials at Ewha Woman's University.

[1] T. L. Makarova, B. Sundqvist, R. Höhne, P. Esquinazi, Y. Kopelevich, P. Scharff, V. A. Davydov, L. S. Kashevarova, A. V. Rakhmanina, *Nature* **2001**, *413*, 716–718.
[2] E. Nakamura, H. Isobe, *Acc. Chem. Res.* **2003**, *36*, 807–815.
[3] R. D. Bolskar, A. F. Benedetto, L. O. Husebo, R. E. Price, E. F. Jackson, S. Wallace, L. J. Wilson, J. M. Alford, *J. Am. Chem. Soc.* **2003**, *125*, 5471–5478.
[4] M. Bendikov, F. Wudl, D. F. Perepichka, *Chem. Rev.* **2004**, *104*, 4891–4945.
[5] Y. Nishibayashi, M. Saito, S. Uemura, S. Takekuma, H. Takekuma, Z. Yoshida, *Nature* **2004**, *428*, 279–280.
[6] H. Isobe, T. Homma, E. Nakamura, *Proc. Natl. Acad. Sci. USA* **2007**, *104*, 14895–14898.
[7] Y. Matsuo, E. Nakamura, *Chem. Rev.* **2008**, *108*, 3016–3028.
[8] T. Kawauchi, J. Kumaki, A. Kitaura, K. Okoshi, H. Kusanagi, K. Kobayashi, T. Sugai, H. Shinohara, E. Yashima, *Angew. Chem. Int. Ed.* **2008**, *47*, 515–519.
[9] A. H. H. Stephens, M. L. H. Green, *Adv. Inorg. Chem.* **1997**, *44*, 1–43.
[10] A. L. Balch, M. M. Olmstead, *Chem. Rev.* **1998**, *98*, 2123–2165.
[11] K. Lee, H. Song, J. T. Park, *Acc. Chem. Res.* **2003**, *36*, 78–86.
[12] Y.-J. Cho, T. K. Ahn, H. Song, K. S. Kim, C. Y. Lee, W. S. Seo, K. Lee, S. K. Kim, D. Kim, J. T. Park, *J. Am. Chem. Soc.* **2005**, *127*, 2380–2381.
[13] B. K. Park, G. Lee, K. H. Kim, H. Kang, C. Y. Lee, M. A. Miah, Y.-K. Han, J. T. Park, *J. Am. Chem. Soc.* **2006**, *128*, 11160–11172.
[14] B. K. Park, C. Y. Lee, J. Jung, J. H. Lim, Y.-K. Han, C. S. Hong, J. T. Park, *Angew. Chem. Int. Ed.* **2007**, *46*, 1436–1439.
[15] S. Zhang, T. L. Brown, Y. Du, J. R. Shapley, *J. Am. Chem. Soc.* **1993**, *115*, 6705–6709.
[16] P. J. Fagan, J. C. Calabrese, B. Malone, *Science* **1991**, *252*, 1160–1161.
[17] R. S. Koefod, M. F. Hudgens, J. R. Shapley, *J. Am. Chem. Soc.* **1991**, *113*, 8957–8958.
[18] P. J. Fagan, J. C. Calabrese, B. Malone, *Acc. Chem. Res.* **1992**, *25*, 134–142.
[19] M. Rasinkangas, T. T. Pakkanen, T. A. Pakkanen, M. Ahlgrén, J. Rouvinen, *J. Am. Chem. Soc.* **1993**, *115*, 4901–4901.
[20] R. E. Douthwaite, M. L. H. Green, A. H. H. Stephens, J. F. C. Turner, *J. Chem. Soc., Chem. Commun.* **1993**, 1522–1523.
[21] I. J. Mavunkal, Y. Chi, S.-M. Peng, G.-H. Lee, *Organometallics* **1995**, *14*, 4454–4456.
[22] A. N. Chernega, M. L. H. Green, J. Haggitt, A. H. H. Stephens, *J. Chem. Soc., Dalton Trans.* **1998**, 755–767.
[23] M. Sawamura, H. Iikura, E. Nakamura, *J. Am. Chem. Soc.* **1996**, *118*, 12850–12851.

[24] H. Iikura, S. Mori, M. Sawamura, E. Nakamura, *J. Org. Chem.* **1997**, *62*, 7912–7913.
[25] Y. Matsuo, A. Iwashita, E. Nakamura, *Organometallics* **2008**, *27*, 4611–4617.
[26] E. G. Gal′pern, A. R. Sabirov, I. V. Stankevich, *Phys. Solid State* **2007**, *49*, 2330–2334.
[27] A. Hirsh, T. Grösser, A. Skiebe, A. Soi, *Chem. Ber.* **1993**, *126*, 1061–1067.
[28] S. Ballenweg, R. Gleiter, W. Kratschmer, *Tetrahedron Lett.* **1993**, *34*, 3737–3740.
[29] S. Ballenweg, R. Gleiter, W. Kratschmer, *J. Chem. Soc., Chem. Commun.* **1994**, 2269–2270.
[30] Y.-H. Zhu, L.-C. Song, Q.-M. Hu, C.-M. Li, *Org. Lett.* **1999**, *1*, 1693–1695.
[31] M. M. Olmstead, K. Maitra, A. L. Balch, *Angew. Chem. Int. Ed.* **1999**, *38*, 231–233.
[32] H.-F. Hsu, J. R. Shapley, *J. Am. Chem. Soc.* **1996**, *118*, 9192–9193.
[33] K. Lee, H.-F. Hsu, J. R. Shapley, *Organometallics* **1997**, *16*, 3876–3877.
[34] K. Lee, J. R. Shapley, *Organometallics* **1998**, *17*, 3020–3026.
[35] H. Song, K. Lee, J. T. Park, M.-G. Choi, *Organometallics* **1998**, *17*, 4477–4483.
[36] J. T. Park, H. Song, J.-J. Cho, M.-K. Chung, J.-H. Lee, I.-H. Suh, *Organometallics* **1998**, *17*, 227–236.
[37] K. Lee, C. H. Lee, H. Song, J. T. Park, H. Y. Chang, M.-G. Choi, *Angew. Chem. Int. Ed.* **2000**, *39*, 1801–1804.
[38] H. Song, Y. Lee, Z.-H. Choi, K. Lee, J. T. Park, *Organometallics* **2001**, *20*, 3139–3144.
[39] K. Lee, Z.-H. Choi, Y.-J. Cho, H. Song, J. T. Park, *Organometallics* **2001**, *20*, 5564–5570.
[40] H. Song, K. Lee, C. H. Lee, J. T. Park, H. Y. Chang, M.-G. Choi, *Angew. Chem. Int. Ed.* **2001**, *40*, 1500–1502.
[41] K. H. Kim, J. Jung, Y.-K. Han, *Organometallics* **2004**, *23*, 3865–3869.
[42] A. D. Becke, *Phys. Rev. A* **1988**, *88*, 3098–3100.
[43] J. P. Perdew, Y. Wang, *Phys. Rev. B* **1992**, *45*, 13244–13249.
[44] D. Andrae, U. Häußermann, M. Dolg, H. Stoll, H. Preuß, *Theor. Chim. Acta* **1990**, *77*, 123–141.
[45] B. Delley, *J. Chem. Phys.* **1990**, *92*, 508–517.
[46] B. Delley, *J. Chem. Phys.* **2000**, *113*, 7756–7764.
[47] K. Morokuma, *J. Chem. Phys.* **1971**, *55*, 1236–1244.
[48] K. Morokuma, *Acc. Chem. Res.* **1977**, *10*, 294–300.
[49] T. Ziegler, A. Rauk, *Theor. Chim. Acta* **1977**, *46*, 1–10.
[50] C. Massera, G. Frenking, *Organometallics* **2003**, *22*, 2758–2765.
[51] K. H. Kim, J. Jung, B. K. Park, Y.-K. Han, J. T. Park, *J. Comput. Chem.* **2007**, *28*, 1100–1106.
[52] H. Song, J. I. Choi, K. Lee, M.-G. Choi, J. T. Park, *Organometallics* **2002**, *21*, 5221–5228.
[53] H. Song, K. Lee, J. T. Park, M.-G. Choi, *J. Organomet. Chem.* **2000**, *599*, 49–56.
[54] H. Song, C. H. Lee, K. Lee, J. T. Park, *Organometallics* **2002**, *21*, 2514–2520.
[55] C. Y. Lee, B. K. Park, H. H. Yoon, C. S. Hong, J. T. Park, *Organometallics* **2006**, *25*, 4634–4642.

Received: January 15, 2010
Published Online: February 24, 2010

